Chinese Journal of Natural Medicines

Structure-guided isolation of anti-neuroinflammatory sesquiterpene coumarins from *Ferula sinkiangensis*

Wen DANG, Tingting GUO, Di ZHOU, Qingqi MENG, Mingxia FANG, Gang CHEN, Bin LIN, Yue HOU, Ning LI

Citation: Wen DANG, Tingting GUO, Di ZHOU, Qingqi MENG, Mingxia FANG, Gang CHEN, Bin LIN, Yue HOU, Ning LI, Structure-guided isolation of anti-neuroinflammatory sesquiterpene coumarins from *Ferula sinkiangensis*, Chinese Journal of Natural Medicines, 2024, 22(7), 643-653. doi: 10.1016/S1875-5364(24)60674-6.

View online: https://doi.org/10.1016/S1875-5364(24)60674-6

Available online at www.sciencedirect.com
ScienceDirect
Chinese Journal of Natural Medicines 2024, **22**(7): 643-653
doi: 10.1016/S1875-5364(24)60674-6
Chinese Journal of Natural Medicines

•Original article•

Structure-guided isolation of anti-neuroinflammatory sesquiterpene coumarins from *Ferula sinkiangensis*

DANG Wen[1Δ], GUO Tingting[1Δ], ZHOU Di[1], MENG Qingqi[2], FANG Mingxia[2], CHEN Gang[1], LIN Bin[3], HOU Yue[2*], LI Ning[1*]

[1] *School of Traditional Chinese Materia Medica, Key Laboratory of Innovative Traditional Chinese Medicine for Major Chronic Diseases of Liaoning Province, Key Laboratory for TCM Material Basis Study and Innovative Drug Development of Shenyang City, Shenyang Pharmaceutical University, Shenyang 110016, China;*
[2] *College of Life and Health Sciences, Northeastern University, Shenyang 110004, China;*
[3] *School of Pharmaceutical Engineering, Shenyang Pharmaceutical University, Shenyang 110016, China*

Available online 20 Jul., 2024

[ABSTRACT] The resin of *Ferula sinkiangensis* has been traditionally utilized for treating gastrointestinal disorders, inflammation, tumors, various cancers, and alopecia areata. The primary bioactive constituents, sesquiterpene coumarins, have demonstrated notable therapeutic potential against neuroinflammation. In this study, a structure-guided fractionation method was used to isolate nine novel sesquiterpene coumarins from the resin of *F. sinkiangensis*. These compounds were characterized and structurally elucidated using comprehensive physicochemical and spectroscopic techniques, including calculated electronic circular dichroism (ECD). Anti-neuroinflammatory assays revealed that compounds **2**, **3**, and **6** significantly inhibited nitric oxide (NO) production in lipopolysaccharide (LPS)-stimulated BV2 microglial cells, with IC_{50} values ranging from 1.63 to 12.25 μmol·L^{-1}.

[KEY WORDS] *Ferula sinkiangensis*; Sesquiterpene coumarins; Structure elucidation; Anti-neuroinflammatory activity
[CLC Number] R284.1, R965 **[Document code]** A **[Article ID]** 2095-6975(2024)07-0643-11

Introduction

Ferula (Apiaceae), a rare traditional medicinal plant, is distributed across Central Asia, the Western Mediterranean, and Northern Africa. Its resin is known as “Awei” in China, “Kama” in Afghanistan, “Sheingho” in Myanmar, and “Asafoetida” in other regions. In China, “Awei” has a medicinal history spanning over 1300 years, primarily used for treating gastrointestinal disorders and various cancers [1]. Additionally, it is employed in treating alopecia areata, malignant inflammatory paralysis, dental issues, and other ailments, particularly in the Xinjiang region.

Neuroinflammation, driven by the overactivation of microglia, plays a critical role in numerous neurodegenerative diseases such as stroke, Alzheimer’s disease, and Parkinsonism. Increasing evidence indicates that overactivated microglia produce various neurotoxic factors, including nitric oxide (NO), tumor necrosis factor-alpha (TNF-α), and interleukin-1 beta (IL-1β), leading to neuronal damage [2, 3]. Therefore, inhibiting microglial hyperactivation is a promising strategy for discovering potential neuroprotective agents. Previous studies have identified sesquiterpene coumarins (SCs) from *F. sinkiangensis* as potent inhibitors of neuroinflammation [4]. SCs, such as kellerin, have demonstrated significant therapeutic potential by reducing infarct volume in middle cerebral artery occlusion (MCAO) rats, indicating their efficacy in treating ischemic stroke *in vivo* [5].

Building on the neuroinflammation inhibitory potential of SCs, we conducted a structure-guided fractionation study on the resin of *F. sinkiangensis*. This process led to the isolation of nine previously undescribed SCs: isobutyryl farnesiferol (**1**), farnesiferone C (**2**), farnesiferol acetate (**3**), ferusingensine I (**4**), ferusingensine J (**5**), ferusingensine L (**6**), ferusingensine M (**7**), ferusingensine N (**8**), and ferusingensine O (**9**) (Fig. 1). We report the isolation and structural elucidation of these novel SCs and their anti-neuroinflammatory effects in lipopolysaccharide (LPS)-induced BV2 microglial

[Received on] 11-Jan.-2024
[Research funding] This work was supported by the National Natural Science Foundation of China (No. U1903122), the Scientific Research Fund of Liaoning Province Education Department (No. LJKZ0945), and the Natural Science Foundation of Liaoning Province (No. 2022-MS-242).
[*]**Corresponding author]** E-mails: houyue@mail.neu.edu.cn (HOU Yue); liningsypharm@163.com (LI Ning)
[Δ]These authors contributed equally to this work.
These authors have no conflict of interest to declare.

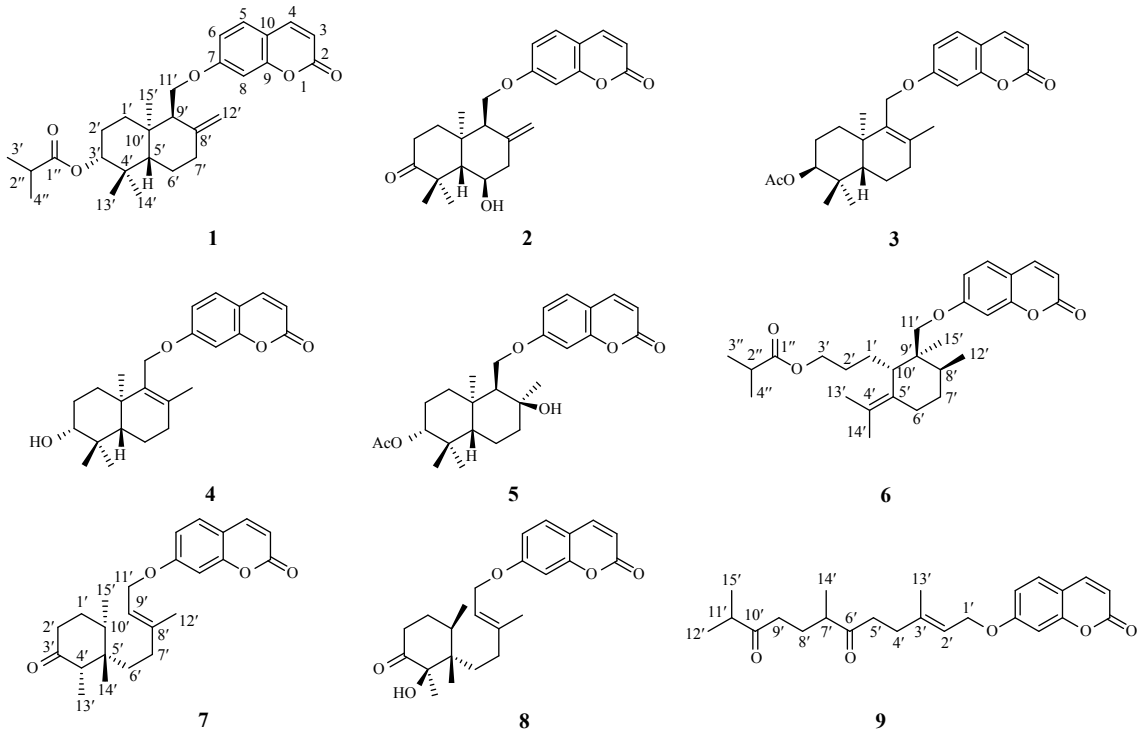

Fig. 1 Structures of compounds 1–9.

cells. Notably, farnesiferone C (**2**), farnesiferol acetate (**3**), and ferusingensine L (**6**) significantly inhibited NO production in LPS-stimulated BV2 cells, with IC_{50} values ranging from 1.63 to 12.25 μmol·L^{-1}.

Results and Discussion

Characteristic MS/MS fragment ions of SCs

To facilitate the rapid identification of SCs in complex mixtures, we detailed the fragmentation pathways of reference compounds, as depicted in Fig. 2A, based on their characteristic ion fragments. SCs can be categorized into three groups: acyclic, monocyclic, and dicyclic umbelliferone-derived SCs. The fragmentation pathways for these groups were elucidated using umbelliprenin, fekrynol, sinkianone, and acetylferukrin as representative examples.

Acyclic umbelliferone-derived SCs exhibit relatively simple cleavage patterns. Diagnostic ions of these SCs often serve as general markers for umbelliferone-derived SCs. For umbelliprenin, the protonated ion at *m/z* 367 produced fragments at *m/z* 205, 163, and 107, resulting from the loss of sesquiterpenes and decarbonylation. The fragment at *m/z* 163 is the most abundant, as it indicates the loss of a sesquiterpene group *m/z* 367. Consequently, the diagnostic ions for umbelliprenin and similar SCs are identified as *m/z* 367→163→107.

The fragmentation of monocyclic SCs, such as fekrynol and sinkianone, involves the cleavage of rings A and B. For fekrynol, the quasimolecular ion at *m/z* 385 $[M + H]^+$ yields fragments at *m/z* 223 $[M - C_9H_6O_3 + H]^+$, 163 $[M - C_{15}H_{26}O - RH + H]^+$, and 107 $[M - C_{15}H_{26}O - RH - 2CO + H]^+$. Additional fragments at *m/z* 205 and 189 result from successive losses of H_2O, while the fragments at *m/z* 149, 135, and 121 stem from the loss of methylene groups. Thus, the diagnostic ions for monocyclic SCs with A-ring cleavage are *m/z* 223→189→149→135→121. For sinkianone, the quasimolecular ion at *m/z* 383 $[M + H]^+$ produces fragments at *m/z* 221, 163, and 107, similar to the A-ring cleavage pattern. The ion at *m/z* 221 further fragments to *m/z* 203 and 119 through the loss of H_2O and A-ring removal. Thus, the diagnostic ions for monocyclic SCs with B-ring cleavage are *m/z* 221→203→119.

In addition, dicyclic SCs exhibit fragmentation patterns similar to monocyclic SCs with A-ring cleavage. For acetylferukrin, fragment ions at *m/z* 147, 133, and 119 result from decarbonylation. The diagnostic ions for identifying dicyclic SCs are *m/z* 223→203→147→133→119.

Based on these fragmentation pathways, we analyzed the resin of *F. Sinikiangensis* using LC-MS (Fig. 2B) [6]. The data revealed a series of compounds that conform to the established fragmentation patterns for SCs, particularly in the middle polar fraction of the resin. By comparing molecular weights with those in the SCs database, we hypothesized that some of these compounds might be novel SCs (Fig. 2C). Given that identical molecular formulas can correspond to multiple chemical structures, it was unclear whether the detected compounds of types A and B were previously known. Since LC-MS data alone cannot resolve this ambiguity, we employed conventional separation methods for the intermediate polar fraction of *F. Sinikiangensis* resin. As a result, we successfully identified a series of previously undescribed compounds, labeled as **1**–**9**, using a variety of analytical tech-

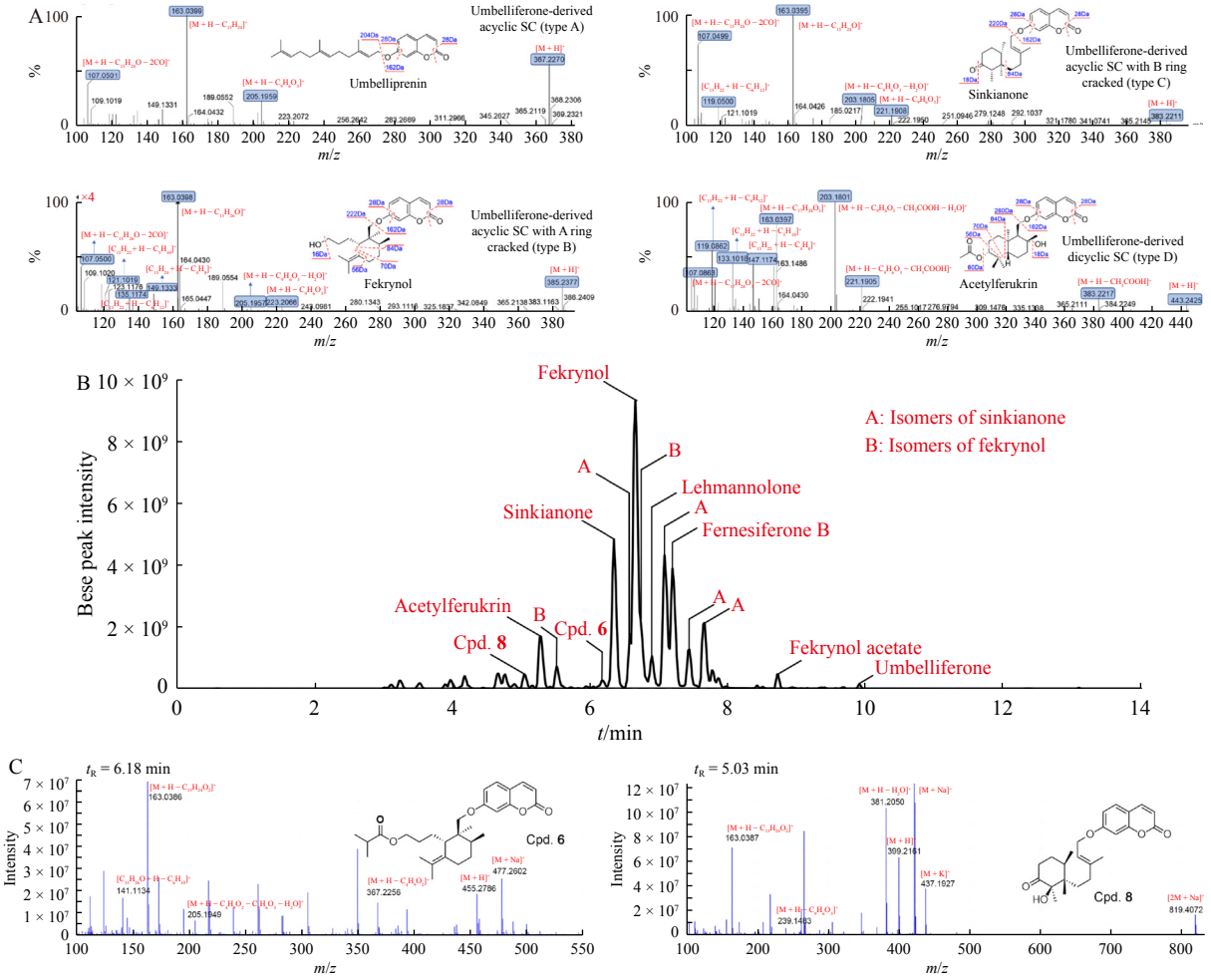

Fig. 2 (A) UPLC-MS/MS spectra and the proposed fragmentation pathways of four representative SCs (umbelliprenin, fekrynol, sinkianone, and acetylferukrin) in positive ion mode. (B) Base peak ion chromatograms from the positive ionization mode of LC-MS of the *F. sinkiangensis* resina chemical extract in the 360−500 range. (C) Positive ESI-MS-Base peak ion chromatograms of compounds 6 and 8, respectively.

niques.

Structural elucidation

Compound **1** was obtained as a white amorphous powder (MeOH). Its molecular formula of $C_{28}H_{36}O_5$ was determined from the molecular ion peak at *m/z* 453.2642 $[M + H]^+$ (Calcd. 453.2641 for $C_{28}H_{37}O_5$) obtained by HR-ESI-MS, indicating 11 degrees of unsaturation.

The ^{1}H NMR spectrum (Table 1) of **1** showed five characteristic protons of 7-*O*-substituted coumarin moiety at δ_H 7.63 (1H, d, J = 9.5 Hz, H-4), 7.36 (1H, d, J = 8.3 Hz, H-5), 6.80 (1H, m, H-8), 6.78 (1H, m, H-6) and 6.24 (1H, d, J = 9.5 Hz, H-3), along with two olefinic protons at δ_H 4.82 (1H, s, Ha -12'), 4.73 (1H, s, Hb -12'), an oxygenated methine group at δ_H 4.48 (1H, m, H-3'), one oxygenated methylene group at δ_H 4.30 (1H, dd, J = 10.0, 6.0 Hz, Ha -11')/4.02 (1H, dd, J = 10.0, 6.0 Hz, Hb -11'), and three tertiary methyl groups at δ_H 1.02 (3H, s, CH_3-15'), 0.92 (3H, s, CH_3-13') and 0.90 (3H, s, CH_3-14'). Moreover, signals at δ_H 2.54 (1H, m, H-2"), δ_H 1.18 (3H, d, J = 7.0 Hz, CH_3-3"), and 1.16 (3H, d, J = 7.0 Hz, CH_3-3") were also observed in the ^{1}H NMR spectrum, indicating the presence of an isobutyryl group. The ^{13}C NMR spectrum of **1** (Table 2) exhibited twenty-eight carbon signals, containing nine carbon signals for characteristic umbelliferone skeleton [δ_C 162.0 (C-7), 161.4 (C-2), 156.0 (C-9), 143.5 (C-4), 128.9 (C-5), 113.2 (C-3), 113.1 (C-6), 112.7 (C-10), and 102.0 (C-8)], and four carbon signals for the isobutyryl group at δ_C 176.9 (C-1"), 34.6 (C-2"), 19.3 (C-3"), and 19.1 (C-4"). The remaining 15 carbon signals indicate the presence of the sesquiterpene fragment, including two olefinic carbon signals at δ_C 146.7 (C-8'), 111.6 (C-12'), and two oxygenated carbon signals at δ_C 80.2 (C-3') and 68.2 (C-11'). These 1D NMR data indicated that **1** was a sesquiterpene coumarin [7]. Furthermore, as the coumarin moiety (7 degrees of unsaturation), one carbonyl group, and one double bond only contributed to 9 degrees of unsaturation, the sesquiterpene moiety of **1** was deduced to be dicyclic. These observations align with a reported dicyclic sesquiterpene coumarin scaffold [8]. The heteronuclear multiple bond correlation (HMBC) of δ_H 4.48 (1H, m, H-3') witho δ_C 176.9 (C-1") suggested the location of the isobutyryl group was at C-3'. The correlations of δ_H 4.82

Table 1 ^{1}H NMR (600 MHz or 400 MHz) data for compounds 1–4 in $CDCl_3$

No.	1	2	3#	4
3	6.24, d (9.5)	6.26, d (9.5)	6.24, d (9.5)	6.23, d (9.5)
4	7.63, d (9.5)	7.63, d (9.5)	7.63, d (9.5)	7.62, d (9.5)
5	7.36, d (8.3)	7.37, d (8.4)	7.37, d (9.3)	7.35, d (9.3)
6	6.81*	6.82, dd (8.4, 2.4)	6.89*	6.83*
8	6.80*	6.81, d (2.4)	6.88*	6.79*
1'*α* (a)	1.72, m	2.08, m	1.68, m	1.69*
1'*β* (b)	1.39, m	1.66, m	1.48, m	1.48*
2'*α* (a)	1.43, m	2.59, m	1.91, m	1.68*
2'*β* (b)	-	2.52, m	1.68, m	1.62*
3'	4.48, m	-	4.70, br. s	3.27 dd (11.3, 4.5)
5'	1.42, m	1.96, d (10.7)	1.69, m	1.22 dd (12.4, 1.8)
6'*α* (a)	1.70, m	3.91, td (10.7, 5.3)	1.66, m	1.73*
6'*β* (b)	-	-	1.54, m	1.54*
7'*α* (a)	2.34, br. d (14.5)	2.62, m	2.17, m	2.15, m
7'*β* (b)	2.06, m	2.23, m	-	
8'	-	-	-	
9'	2.22, t (5.9)	2.33, t (6.0)	-	
11'a	4.30, dd (10.0, 6.0)	4.31, dd (9.8, 6.8)	4.56, d (10.0)	4.53, d (10.0)
11'b	4.02, dd (10.0, 6.0)	4.15, dd (9.8, 6.3)	4.42, d (10.0)	4.38, d (10.0)
12'a	4.82, s	4.95, t (2.0)	1.72, s	1.68, s
12'b	4.73, s	4.87, t (2.0)	-	
13'	0.92, s	1.36, s	0.90, s	1.03, s
14'	0.90, s	1.33, s	0.94, s	0.82, s
15'	1.02, s	0.97, s	1.06, s	1.02, s
2''	2.54, m	-	2.07, s	
3''	1.16, d (7.0)	-	-	
4''	1.17, d (7.0)			

* Overlapped signals; # Tested at 400 MHz.

(1H, br. s, H_a-12') and 4.73 (1H, br. s, H_b-12') with δ_C 56.7 (C-9') and 32.4 (C-7') and of δ_H 0.92 (3H, s, CH_3-13') and 0.90 (3H, s, CH_3-14') with δ_C 80.2 (C-3'), 38.2 (C-4'), and 46.8 (C-5') indicated that the terminal double bond was situated at C-8', and CH_3-13' and CH_3-14' was located at C-4', respectively. The CH_3-15' was situated at C-10' and was supported by the HMBCs of δ_H 1.02 (3H, s, CH_3-15') with δ_C 56.7 (C-9'), 46.8 (C-5'), and 34.6 (C-1') (Fig. 3). The relative configuration of **1** was deduced from the NOESY spectrum (Fig. 4). The correlations between H-3'/H-5'/H_2-11' and CH_3-14'/CH_3-15'/H-9' established an *β*-orientation for H_2-11', H-3', and CH_3-13', and an *α*-orientation for H-9', CH_3-14', and CH_3-15'. Furthermore, through comparative experiments and calculated ECD spectra, the absolute configuration of **1** was further determined as 3'*R*,5'*S*,9'*S*,10'*R* (Fig. 5). The structure of **1** was identified as isobutyryl farnesiferol.

Compound **2** was assigned the molecular formula $C_{24}H_{28}O_5$, with four carbon atoms and eight hydrogen atoms mass units less than that of **1**. The 1D NMR spectra of **2** indicated a structure similar to those of **1**, except that **2** lacks isobutyl signals and has additional hydroxyl and carbonyl substituents. Additionally, the chemical shift of H-6' changed from δ_H 1.70 (2H, m) to δ_H 3.70 (1H, td, J = 10.7, 5.3 Hz), indicating that the hydroxyl group is located at C-6' in **2**, which was further confirmed by the HMBC spectrum (Fig. 3). In the NOESY spectrum, the correlations of H-5'/H_2-11' indicated they were assigned as *β*-orientations, while the correlations of H-6'/CH_3-15'/H-9' showed their *α*-orientations (Fig. 4). A comparison of calculated and experimental ECD spectra substantiated the absolute configuration of **2**. Based on this comparison, the absolute configuration of **2** was determined to be **2** is 5'*S*,6'*R*,9'*S*,10'*S* (Fig. 5). Thus, the structure of **2** was identified as farnesiferone C.

Compound **3** was assigned the molecular formula $C_{26}H_{32}O_5$, with 11 degrees of unsaturation. It had two carbon and four fewer hydrogen atoms than **1**. Compared with that of **1**, the 1D NMR spectrum of **3** showed the presence of acetoxyl and hydroxyl groups without isobutyryl groups (Tables 1 and 2). Additionally, proton and carbon signals were assigned values based on HSQC and HMBC data. The HMBC

Table 2 ^{13}C NMR (150 MHz or 100 MHz) data for compounds **1**–**9** in $CDCl_3$

No.	1	2	3	4	5[#]	6	7	8	9
2	161.4	161.2	161.4	161.4	161.4	161.4	161.4	161.4	161.3
3	113.2	113.5	113.2	113.1	113.1	112.9	113.2	113.1	113.1
4	143.5	143.5	143.5	143.6	143.6	143.6	143.6	143.6	143.5
5	128.9	129.0	128.8	128.8	128.9	128.7	128.8	128.8	128.8
6	113.1	113.2	113.3	113.3	113.2	113.3	113.3	113.4	113.2
7	162.1	161.8	162.6	162.6	162.6	163.1	162.2	162.3	162.1
8	102.0	101.8	101.6	101.5	102.0	101.3	101.7	101.8	101.6
9	156.0	156.0	156.1	156.0	156.0	156.1	156.0	156.0	155.9
10	112.7	112.9	112.6	112.6	112.7	112.4	112.6	112.6	112.6
1'	34.6	33.6	30.2	34.7	35.1	26.9	29.9	30.8	65.4
2'	22.9	34.3	23.3	27.7	23.9	23.3	37.0	36.3	118.9
3'	80.2	217.2	77.7	78.8	80.7	64.9	214.9	215.0	141.1
4'	38.2	47.7	36.9	38.9	38.1	125.3	51.5	81.3	33.0
5'	46.8	53.0	45.8	50.7	47.4	130.3	42.1	47.3	39.0
6'	24.1	70.3	18.4	18.7	19.9	24.6	34.2	35.4	213.2
7'	32.4	42.9	33.7	34.1	39.1	32.2	32.8	35.1	45.5
8'	146.7	143.6	136.0	136.0	72.3	35.0	142.8	143.8	26.4
9'	56.7	54.8	135.4	135.2	59.2	40.9	118.6	118.0	37.4
10'	37.7	37.9	37.9	37.9	37.7	43.1	33.5	37.4	214.2
11'	68.2	67.9	64.7	64.7	67.0	71.9	65.6	65.7	40.9
12'	111.6	113.7	19.7	19.5	32.4	16.2	17.1	17.1	18.3
13'	17.0	31.3	27.8	28.2	28.3	20.4	10.3	10.3	17.0
14'	28.5	21.9	21.8	15.5	16.6	20.3	20.6	20.6	16.4
15'	22.3	21.5	20.8	20.9	24.8	22.6	14.8	14.8	18.3
1"	176.9	-	170.9		171.0	177.4			
2"	34.6		21.5		21.4	34.2			
3"	19.3	-	-			19.2			
4"	19.1					19.2			

[#] Tested at 100 MHz.

of δ_H 4.70 (1H, br. s, H-3') with δ_C 170.9 (C-1") indicated that the acetoxyl group was located at C-3'. Besides, the HMBC of δ_H 1.72 (3H, s, CH_3-12') with δ_C 135.4 (C-9') and 33.4 (C-7') demonstrated that CH_3-12' was in conjunction with C-8' (Fig. 3). Through the NOE correlation of H-3'/CH_3-14'/CH_3-15' and H-5'/CH_3-13', the relative configuration of **3** was determined to be 3'R^*,5'R^*,10'S^* (Fig. 4). By comparing the experimental and calculated ECD spectra, the absolute configuration of **3** was further confirmed as 3'*R*,5'*R*,10'*S* (Fig. 5). Thus, the structure of **3** was identified as farnesiferol acetate.

Compound **4** exhibited a molecular formula $C_{24}H_{30}O_4$ with 10 degrees of unsaturation. Compared with the 1D NMR data of **3**, the acetyl group of **4** was replaced by the hydroxyl group, which was supported by the HMBC of δ_H 3.27 (H-3') with δ_C 34.7 (C-1'), 27.7 (C-2'), and 38.9 (C-4') (Fig. 3). The NOESY correlations between CH_3-14'/CH_3-15' and H-3'/H-5'/CH_3-13' indicated that H-3', H-5', CH_3-13' were β-oriented, and CH_3-13', H-5' were α-oriented (Fig. 4). The relative configuration of **4** was suggested to be 3'R^*,5'S^*,10'R^*. A comparison between calculated and experimental ECD spectra was carried out to validate its absolute configuration. As shown in Fig. 5, (3'*R*,5'*S*,10'*R*)-**4** matched well with the experimental curve, revealing the absolute configuration as (3'*R*,5'*S*,10'*R*)-**4** for which the name was proposed as ferusingensine I.

Compound **5** had a molecular formula of $C_{26}H_{34}O_6$, according to a molecular ion peak at *m/z* 443.2436 $[M + H]^+$ (Calcd. 443.2428 for $C_{26}H_{35}O_6$) from HR-ESI-MS data, which was 18 Da higher than that of **3**. A comparison of 1D NMR data and molecular formulas of **5** and **3** (Tables 2 and 3) showed that **5** contained a hydroxyl group while lacking one double bond present in **3**. The HMBC spectrum indicated the correlations of δ_H 4.53 (H_a-11')/4.38 (H_b-11') with δ_C 72.3 (C-8') and δ_H 1.51 (CH_3-12') with δ_C 39.1 (C-7'), 59.2 (C-9'), confirming that the hydroxyl group was located at C-8' (Fig. 3). The NOE correlations between H-3'/H-5', H-3'/CH_3-13', CH_3-15'/CH_3-12'/CH_3-14' clearly indicated that CH_3 -12', CH_3-14', and CH_3-15' were α-oriented, while H-3', H-5', CH_3-13', and H_2-11' were β-oriented (Fig. 4), and the relative configuration was determined as 3'R^*,5'S^*,8'S^*,9'S^*,10'R^*. The absolute configurations of **5** were suggested as 3'*R*,5'*S*,8'*S*,9'*S*,10'*R* by comparison with the calculated ECD (Fig. 5). Therefore, compound **5** was identified as ferusingensine J.

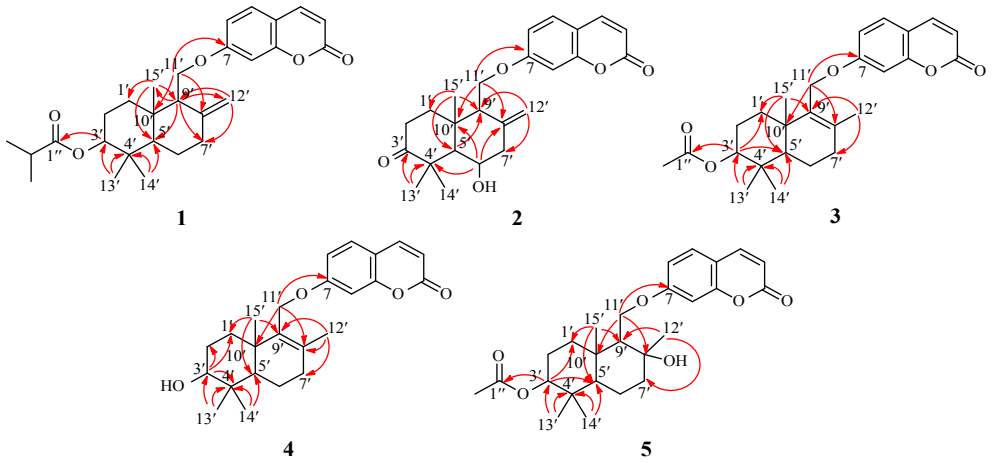

Fig. 3 Key HMBCs ( ) of compounds 1–5.

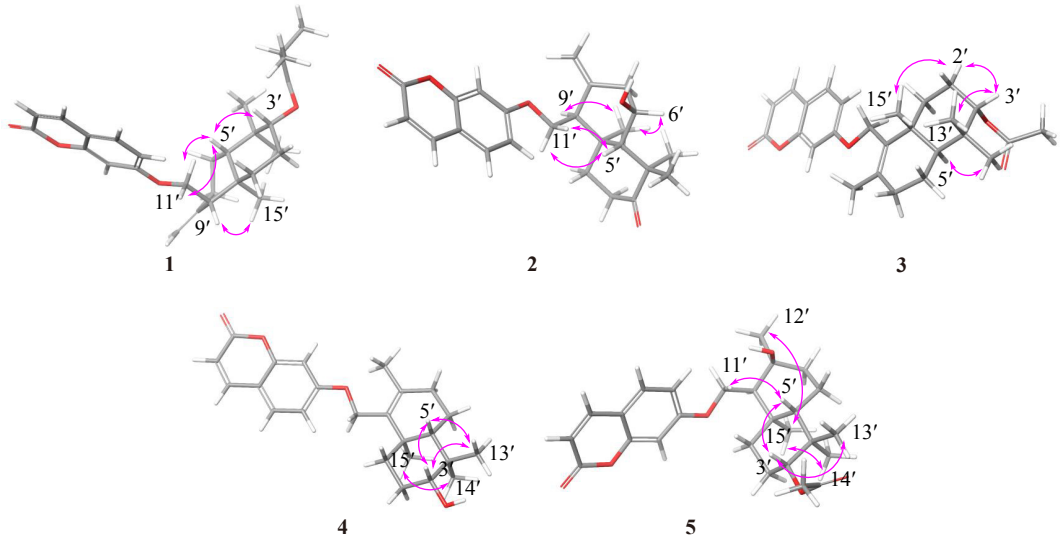

Fig. 4 Key NOESY ( ) correlations of compounds 1–5.

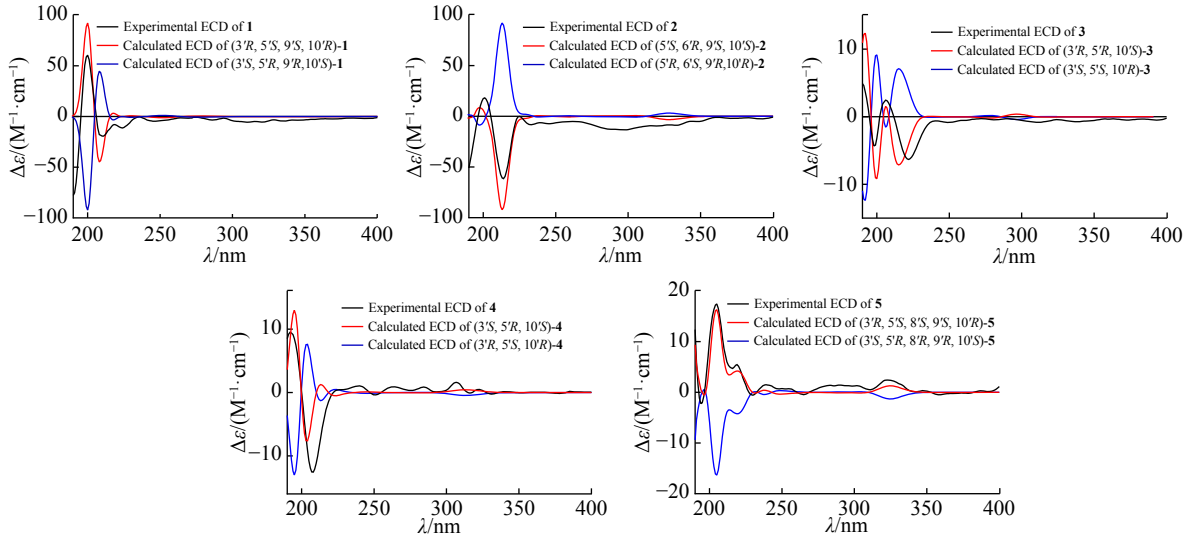

Fig. 5 Comparison of experimental and calculated ECD spectra of compounds 1–5.

Compound **6** had a molecular formula of $C_{28}H_{38}O_5$ according to a molecular ion peak at *m/z* 453.2664 $[M - H]^-$ (Calcd. 453.2646 for $C_{28}H_{37}O_5$) by HR-ESI-MS, indicating 10 degrees of unsaturation. The ^{1}H NMR spectrum (Table 3) revealed the presence of two oxygenated methylene groups at δ_H 4.06 (2H, m, H-3'), 3.87 (1H, d, J = 8.2 Hz, H_a-11')/3.68 (1H, d, J = 8.2 Hz, H_b-11'), and six methyl groups at δ_H 1.62 (3H, d, J = 0.4 Hz, CH_3-14'), 1.45 (3H, d, J = 1.7 Hz, CH_3-13'), 1.18 (6H, d, J = 7.0 Hz, CH_3-3", CH_3-4"), 1.11 (3H, s, CH_3-15'), and 0.90 (3H, d, J = 7.0 Hz, CH_3-12'). The ^{13}C NMR spectrum (Table 2) indicated a characteristic umbelliferone skeleton. Additionally, 15 carbon signals indicated the presence of a sesquiterpene fragment, including two olefinic carbon signals at δ_C 130.3 (C-5'), 125.3 (C-4') and two oxygenated carbon signals at δ_C 71.9 (C-11') and 64.9 (C-3'). Besides, the remaining four carbon signals at δ_C 177.4 (C-1"), 34.2 (C-2"), 19.2 (C-3"), and 19.2 (C-4") elucidated the presence of isobutyryl group, corresponding to the three proton signals at δ_H 2.54 (1H, m, H-2"), 1.18 (3H, d, J = 7.0 Hz, CH_3-3"), and 1.16 (3H, d, J = 7.0 Hz, CH_3-4") observed in the ^{1}H NMR spectrum above. Combining the 1D NMR data with the degree of unsaturation, it can be speculated that **6** was a monocyclic SC.

In the HMBC spectrum of **6** (Fig. 6), the correlations of δ_H 4.06 (2H, m, H-3') with δ_C 177.4 (C-1") suggested the location of the isobutyryl group at C-3'. The correlations of δ_H 0.90 (CH_3 -12') with δ_C 32.2 (C-7'), 35.0 (C-8'), and 40.9 (C-9') and of δ_H 1.11 (CH_3 -15') with δ_C 35.0 (C-8'), 40.9 (C-9'), 43.1 (C-10'), and 71.9 (C-11') indicated that CH_3-12' and CH_3-15' were located at C-8' and C-10', respectively. The CH_3-13'/CH_3-14' were located at C-4' was supported by the HMBC of δ_H 1.45 (CH_3 -13') and 1.62 (CH_3 -14') with δ_C 125.3 (C-4') and 130.3 (C-5'). These HMBCs established the planar structure of the sesquiterpene unit in **6**. The NOE correlations between CH_3-12'/ H_b-11', H-10'/ H_a-11', and CH_3-15'/ H-8'/ H-1') established an β-orientation for H_2-11' and CH_3-13', and an α-orientation for H_2-1' and CH_3-15' (Fig. 7). Thus, the relative configuration of compound **6** was established as 8'S^*,9'S^*,10'S^*. The absolute configuration was determined as 8'*S*,9'*S*,10'*S* by comparing the experimental and calculated ECD spectrum (Fig. 8). Therefore, the structure of **6** was identified as ferusingensine L.

Compound **7** was determined to have a molecular formula of $C_{24}H_{30}O_4$ based on the ion peak at *m/z* 405.2046 $[M + Na]^+$ (Calcd. 405.2036 for $C_{24}H_{30}O_4Na$), indicating 10 degrees of unsaturation. The ^{1}H NMR spectrum (Table 3) revealed several key features: an olefinic proton at δ_H 5.46 (1H, t, J = 6.5 Hz, H -9'); an oxygenated methylene group at δ_H 4.57 (2H, d, J = 6.5 Hz, H_2-11'), and four methyl groups at δ_H 1.74 (3H, s, CH_3-12'), 1.03 (3H, d, J = 6.8 Hz, CH_3-15'), 1.02 (3H, d, J = 7.0 Hz, CH_3-13'), and 0.88 (3H, s, CH_3-14'). The ^{13}C NMR spectrum (Table 2) indicated the presence of a characteristic umbelliferone skeleton. Furthermore, 15 carbon signals indicated the presence of a sesquiterpene fragment, including two olefinic carbons at δ_C 142.8 (C-8'), 118.6 (C-9'), one carbonyl signal at δ_C 214.9 (C-3'), and one oxygenated carbon signals at δ_C 65.6 (C-11'). Combining the 1D NMR data with the degree of unsaturation, it can be speculated that **7** was a monocyclic SC. The HMBCs of δ_H 1.89 (H, m, H_α-1'), 1.63 (1H, m, H_β-1'), 1.02 (3H, s, CH_3-13'), and 0.88 (3H, s, CH_3-14') with δ_C 214.9 (C-3') determined that the carbonyl group was located at C-3'. δ_H 1.74 (CH_3-12') related to δ_C 32.8 (C-7'), 142.8 (C-8'), 118.6 (C-9') indicating that CH_3-12' was at C-8' (Fig. 6). Besides, the correlations from δ_H 1.02 (CH_3-13') to δ_C 214.9 (C-3'), 51.5 (C-4'), 42.1 (C-5') demonstrated that CH_3-13' was located at C-4'. The correlations from δ_H 0.88 (CH_3-14') to δ_C 51.5 (C-4'), 42.1 (C-5'), and 34.2 (C-6') indicated the position of CH_3-14' was at C-5'. The position of CH_3-15' at C-10' was supported by the correlations from δ_H 1.03 (CH_3 -15') to δ_C 29.9 (C-1'), 33.5 (C-10'), and 42.1 (C-5'). The correlations from δ_H 4.57 (H_2-11') to δ_C 142.9 (C-8'), 119.3 (C-9'), and 162.2 (C-7) revealed that the double bond was at C-8/C-9. The relative configuration of **7** was confirmed as 4'S^*,5'S^*,10'S^* by the cross-peaks of H-4'/CH_3-14'/H-10', H-6'/CH_3-13'/CH_3-15' in the NOESY spectrum (Fig. 7). The ECD spectrum of **7** was calculated, and the results showed that the calculated ECD spectrum of 4'*S*,5'*S*,10'*S* closely matched the experimental results (Fig. 8), and the structure of **7** was defined as ferusingensine M.

Compound **8** was determined to have a molecular formula of $C_{24}H_{30}O_5$ based on the ion peak at *m/z* 819.4074 $[2M + Na]^+$ (Calcd. 819.4077 for $C_{48}H_{60}O_{10}Na$). Compared with **7**, the molecular weight of **8** is 16 Da more. Detailed analysis of the ^{13}C NMR data of **8** (Table 2) exhibited high similarity to that of **8**, except for the presence of oxygenated carbon signals at δ_C 81.3 at C-4' in **8** but absent in **7**. This hypothesis was supported by the HMBCs of δ_H 1.38 (CH_3 -13'), 0.69 (CH_3 -14'), and 2.01 (H-10') with δ_C 81.3 (C-4') (Fig. 6). The relative configuration of **8** was indicated as 4'R^*,5'S^*,10'S^* by the cross-peaks of CH_3-13'/H_2-6', CH_3-13'/H-10', and CH_3-14'/CH_3-15' in the NOESY spectrum (Fig. 7). Based on the above speculation, the relative configuration of 8 was identified as 4'R^*,5'S^*,10'S^*. Subsequently, the absolute configurations of **8** were suggested as 4'*R*,5'*S*,10'*S* by comparison of the calculated ECD (Fig. 8). Thus, compound **8** was identified as ferusingensine N.

Compound **9** was determined to have a molecular formula of $C_{24}H_{30}O_5$ based on an ion peak at *m/z* 399.2175 $[M + H]^+$ (Calcd. 399.2166 for $C_{24}H_{31}O_5$), indicating an index of hydrogen deficiency of 10. The ^{1}H NMR spectrum (Table 3) revealed an olefinic proton at δ_H 5.44 (1H, t, J = 6.5 Hz, H_a-12'), an oxygenated methylene group at δ_H 4.55 (2H, d, J = 6.5 Hz, H-1'), and four methyl groups at δ_H 1.74 (3H, s, CH_3-13'), 1.05 (3H, overlap, CH_3-14'), 1.04 (3H, overlap, CH_3-15'), and 1.04 (3H, overlap, CH_3-12'). The ^{13}C NMR spectrum indicated a characteristic umbelliferone skeleton. Furthermore, 15 carbon signals indicated the presence of a sesquiterpene fragment, including two olefinic carbon signals at δ_C 141.1 (C-3') and 118.9 (C-2') and two carbonyl carbon signals at δ_C 214.6 (C-10') and 213.2 (C-6'). Combining the 1D

Table 3 ^{1}H NMR (600 MHz or 400 MHz) data for compounds 5–9 in $CDCl_3$

No.	5[#]	6	7	8	9
3	6.23, d (9.5)	6.23, d (9.5)	6.23, d (9.4)	6.24, d (9.5)	6.21, d (9.5)
4	7.63, d (9.5)	7.62, d (9.5)	7.63, d (9.4)	7.63, d (9.5)	7.61, d (9.5)
5	7.36, d (8.8)	7.34, d (8.6)	7.35, d (8.6)	7.36, d (8.6)	7.34, d (8.6)
6	6.83, dd (8.8, 2.2)	6.81, dd (8.6, 2.3)	6.84, dd (8.6, 2.3)	6.86, dd (8.6, 2.4)	6.81, dd (8.6, 2.3)
8	6.88, d (2.2)	6.75, d (2.3)	6.81, d (2.3)	6.82, d (2.4)	6.77, d (2.3)
1'*α*(a)	1.69*	1.50*	1.89*	1.83, m	4.55, d (6.5)
1'*β*(b)	1.42*	1.40*	1.63, m	1.59*	
2'*α*	1.69*	1.53*	2.41*	2.63, m	5.44, t (6.5)
2'*β*			2.30, m	2.41*	
3'*α*	4.45, m	4.06, m			
3'*β*					
4'			2.41*		2.31, t (7.6)
5'	1.47*				2.59, m
6'*α*(a)	1.70*	2.50, m	1.39, m	1.61*	
6'*β*(b)	1.45*	1.89*			
7'*α*(a)	1.75*	1.58, m	1.99*	2.39*	2.53, m
7'*β*(b)	1.59*	1.21*	1.92*	2.15, m	
8'a		1.84*			1.59, m
8'b					1.89, m
9'	1.66*		5.46, t (6.5)	5.48, t (6.5)	2.40, m
10'		2.91, dd (10.5, 3.1)	1.95*	2.01, m	
11'a	4.52, dd (10.0, 1.9)	3.88, d (8.3)	4.57, d (6.5)	4.60, d (6.5)	2.57, m
11'b	4.25, dd (10.0, 5.0)	3.69, d (8.3)			
12'	1.51, s	0.90, d (7.0)	1.74, s	1.78, s	1.04*
13'	0.91, s	1.45, d (1.7)	1.02, d (7.0)	1.38, s	1.74 s
14'	0.88, s	1.62, d (0.4)	0.88, s	0.69, s	1.05*
15'	1.18, s	1.11, s	1.03, d (6.8)	0.94, d (6.7)	1.04*
2''		2.55, m			
3''		1.18, d (7.0)			
4''		1.18, d (7.0)			

* Overlapped signals; # Tested at 400 MHz.

NMR data with the degree of unsaturation, it can be speculated that **9** was an acyclic SC. The HMBCs of δ_H 1.74 (CH_3-13') with δ_C 118.9 (C-2'), 141.1 (C-3'), and 33.0 (C-4') and of δ_H 1.05 (CH_3-14') with δ_C 213.2 (C-6'), 45.5 (C-7'), and 26.4 (C-8') indicated that CH_3-13' and CH_3-14' were located at C-3' and C-7', respectively (Fig. 6). The CH_3-12'/ CH_3-15' were located at C-11' was supported by the correlations of δ_H 1.04 (CH_3 -12') and 1.04 (CH_3 -15') with δ_C 40.9 (C-11') and 214.2 (C-10'). The ECD spectrum of **9** was calculated, and the results showed that the calculated ECD spectrum of 7'*S* closely matched the experimental results (Fig. 8), and the structure of **9** was defined as (7'*S*)-ferusingensine O.

Anti-neuroinflammatory activities of SCs

The model of BV2 microglia cells activated by LPS was established to evaluate the anti-neuroinflammatory activities of all SCs by Griess method. The cell viability assay (Table S1) showed that survival rates of BV2 cells treated with **2** and **3** at a concentration of 100 μmol·L^{-1} and **6** at a concentration of 30 μmol·L^{-1} were over 90%. Compounds **2**–**3**, **6** showed inhibitory activity in NO production with IC_{50} values of 1.63−15.55 μmol·L^{-1} (Table 4, Fig. 9), among which farnesiferol acetate (**3**) showed the most potent inhibitory effect with IC_{50} value at 1.63 μmol·L^{-1}.

Material and Methods

General procedures

A range of instruments and materials were utilized in this study. UV spectra were detected using a Shimadzu UV-2600i spectrophotometer (Shimadzu Co., Ltd., Shanghai, China), while IR spectra were obtained with a GangDong FTIR-650 FT-IR Spectrometer (Tianjin Gangdong SCI. & TECH Co., Ltd., Tianjin, China). High-resolution electrospray ionization mass spectrometry (HR-ESI-MS) data were acquired with a Bruker microTOF-Q mass spectrometer (Bruker Daltonics Inc., Beijing, China). For nuclear magnetic resonance (NMR) analysis, 1D and 2D spectra were recorded using Bruker-AV-400 and Bruker-AV-600 spectrometers (Bruker Daltonics Inc., Beijing, China). Optical rotations were measured with

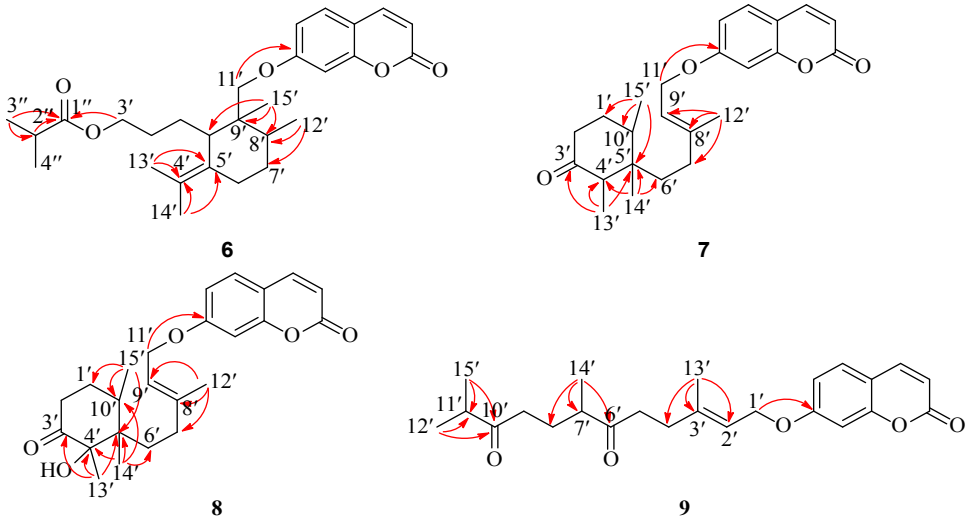

Fig. 6 Key HMBC ( ) correlations of compounds 6–9.

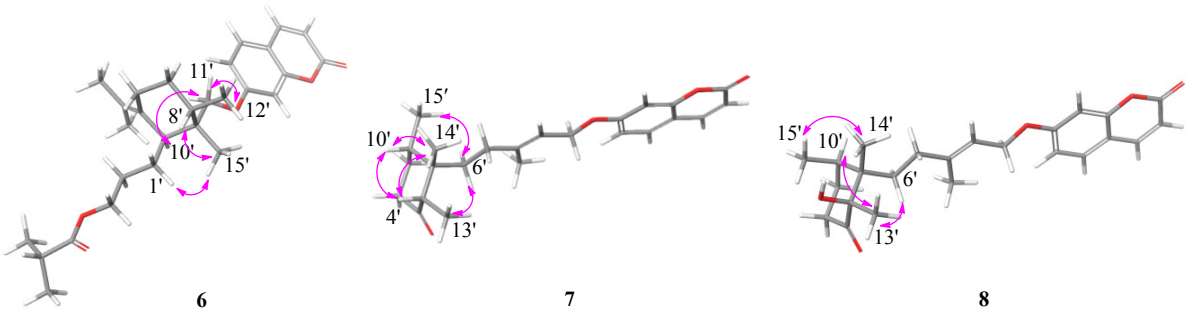

Fig. 7 Key NOESY ( ) correlations of compounds 6–8.

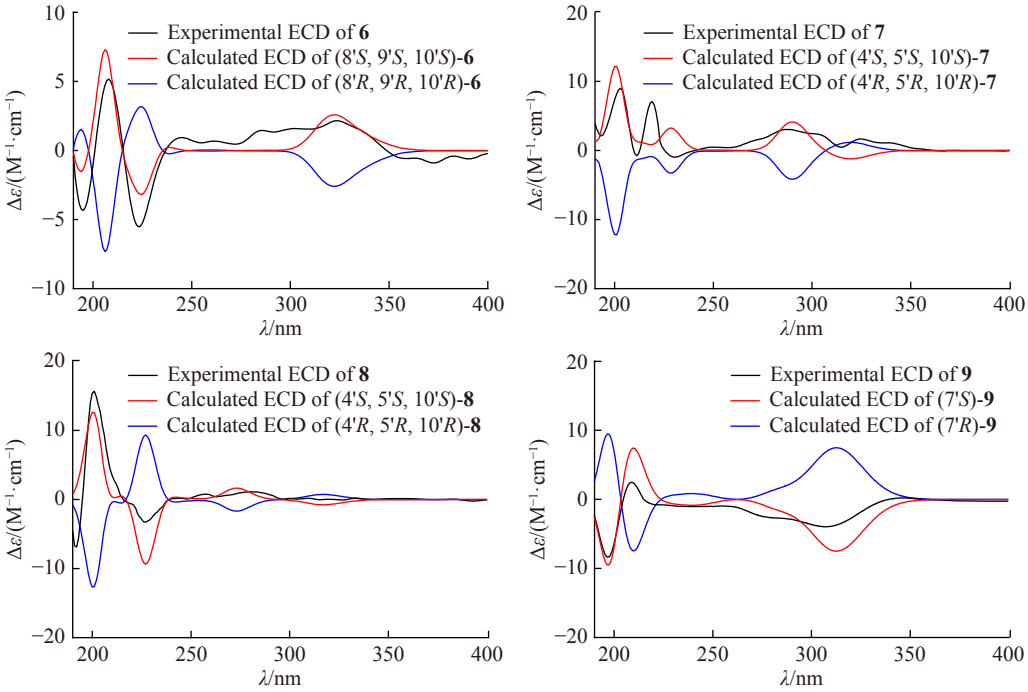

Fig. 8 Comparison of experimental and calculated ECD spectra of compounds 6–9.

Table 4 Effects of SCs purified from *F. sinkiangensis* on NO production in LPS-activated BV2 microglia cells (Mean ± SEM, *n* = 3)

Compounds	IC_{50}/(μmol·L^{-1}) [a]
2	12.25 ± 2.66
3	1.63 ± 2.64
6	4.67 ± 2.64
Minocycline [b]	12.19 ± 1.74

Compounds **1**, **7**, and **8** showed NO inhibitory activity at tested concentrations (1, 10, 30, 100 μmol·L^{-1}); compounds **4**, **5**, and **9** showed cytotoxicities at affected concentrations. [a] 50% Inhibitory concentration after 24 h of drug treatment; [b] Minocycline was used as a positive control.

an Anton Paar MCP200 (Anton Paar Trading Co., Ltd., Shanghai, China), and circular dichroism (CD) spectra were obtained using a Bio-Logic Science MOS-450 circular dichroism spectrometer (DHS Instruments Co., Ltd., Dalian, China). Semi-preparative high-performance liquid chromatography (HPLC) was performed using a YMC ODS C_{18} column (5 μm, 10 mm × 250 mm, ODS-A; YMC Co., Ltd., Shanghai, China) equipped with a Shimadzu SPD-20A UV-VIS detector (Shimadzu Co., Ltd., Shanghai, China). Column chromatography was conducted using silica gel (200−300 mesh, Qingdao Marine Chemical Inc., Qingdao, China) and ODS gel (YMC Co., Ltd., Shanghai, China). All reagents were sourced from Tianjin DaMao Chemical Company (Tianjin, China). NMR spectra were processed using Bruker TopSpin software (Bruker Daltonics Inc., Beijing, China). Dulbecco's Modified Eagle Medium (DMEM) was purchased from Gibco BRL (Grand Island, NY, USA). Lipopolysaccharide (LPS, *E. coli* 055 : B5) and MTT were obtained from Sigma Chemical Co. (St. Louis, MO, USA). Fetal calf serum was sourced from Clark Bio (Richmond, VA, USA), and 96-well cell culture plates were purchased from Thermo Fisher Scientific Inc. (Shanghai, China).

Plant material

The resin of *F. sinkiangensis* was collected in Yining, Xinjiang Province, China, in June 2016. Species authentication was conducted by Dr. PAN Yingni from the School of Traditional Chinese Materia Medica at Shenyang Pharmaceutical University. Voucher specimens have been deposited at Shenyang Pharmaceutical University under Registration No. 20160629.

Liquid chromatography-mass spectrometry (LC-MS) analysis

LC-MS (ESI source) experiments were performed using a Waters ACQUITY UPLC^{TM} system, which includes a Waters Micromass Ultra Performance LC and a Waters Xevo^{TM} G2 Q-TOF mass spectrometer. The column used was an ACQUITY UPLCHSS T3 (100 mm × 2.1 mm, 1.8 μm). The elution program began with an isocratic elution of 40% acetonitrile in water (containing 0.1% formic acid) for 2 min, followed by a linear gradient from 40% to 99% acetonitrile in water over 1−12 min, at a flow rate of 0.4 mL·min^{-1}. All samples were analyzed under these conditions.

Extraction and Isolation

The resin of *F. sinkiangensis* (1 kg) was extracted with 95% ethanol using the same method as in previous studies [9]. Detailed extraction and isolation procedures are provided in the Supporting Information section "S-Extraction and Isolation".

*Isobutyryl farnesiferol (**1**)*: white amorphous powder; $[\alpha]_D^{20}$ −27.3 (*c* 0.50, MeOH); the ^{1}H and ^{13}C NMR ($CDCl_3$) data are presented in Tables 1 and 2; the HR-ESI-MS at *m/z* 453.2642 $[M + H]^+$ (Calcd. 453.2641 for $C_{28}H_{37}O_5$).

*Farnesiferone C (**2**)*: white amorphous powder; $[\alpha]_D^{20}$ −56.0 (*c* 0.45, MeOH); the ^{1}H and ^{13}C NMR ($CDCl_3$) data are detailed in Tables 1 and 2; the HR-ESI-MS at *m/z* 397.2015 $[M + H]^+$ (Calcd. 397.2015 for $C_{24}H_{29}O_5$).

*Farnesiferol acetate (**3**)*: white amorphous powder; $[\alpha]_D^{20}$ −34.2 (*c* 0.26, MeOH); the ^{1}H and ^{13}C NMR ($CDCl_3$) data are provided in Tables 1 and 2; the HR-ESI-MS at *m/z* 425.2337 $[M + H]^+$ (Calcd. 425.2328 for $C_{26}H_{33}O_5$).

*Ferusingensine I (**4**)*: white amorphous powder; $[\alpha]_D^{20}$ −63.91 (*c* 0.50, MeOH); the ^{1}H and ^{13}C NMR ($CDCl_3$) data are shown in Tables 1 and 2; the HR-ESI-MS at *m/z* 405.2046 $[M + Na]^+$ (Calcd. 405.2036 for $C_{24}H_{30}O_4Na$).

*Ferusingensine J (**5**)*: white amorphous powder; $[\alpha]_D^{20}$ −5.61 (*c* 0.41, MeOH); the ^{1}H and ^{13}C NMR ($CDCl_3$) data are shown in Tables 2 and 3; the HR-ESI-MS *m/z* 443.2436 $[M + H]^+$ (Calcd. 443.2428 for $C_{26}H_{35}O_6$).

*Ferusingensine L (**6**)*: white amorphous powder; $[\alpha]_D^{20}$ −10.16 (*c* 0.62, MeOH); the ^{1}H and ^{13}C NMR ($CDCl_3$) data

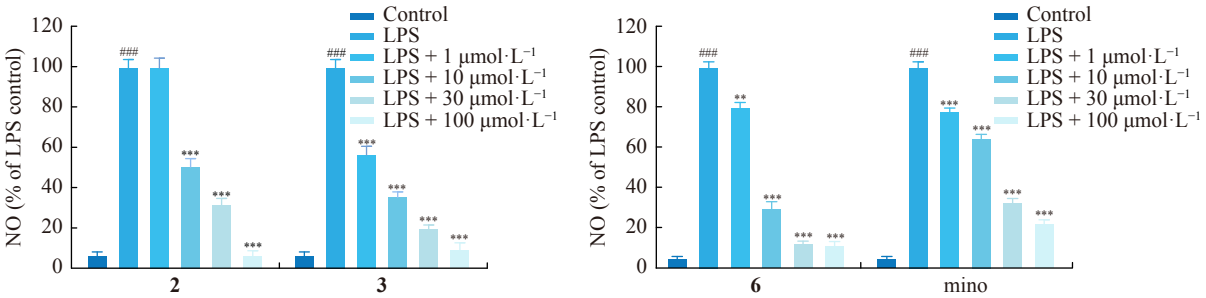

Fig. 9 Anti-neuroinflammatory effects on NO production of active SCs identified from the resin of *F. sinkiangensis* in LPS-induced BV2 microglia (mean ± SEM, *n* = 3). $^{**}P < 0.01$, $^{***}P < 0.001$ *vs* LPS; $^{\#\#\#}P < 0.001$ *vs* Control. NO: nitric oxide, LPS: lipopolysaccharide, mino: minocycline.

are provided in Tables 2 and 3; the HR-ESI-MS at *m/z* 453.2664 $[M-H]^-$ (Calcd. 453.2646 for $C_{28}H_{37}O_5$).

Ferusingensine M (7): white amorphous powder; $[\alpha]_D^{20}$ +5.61 (*c* 0.82, MeOH); the ^1H and ^{13}C NMR ($CDCl_3$) data are shown in Tables 2 and 3; the HR-ESI-MS at *m/z* 405.2046 $[M+Na]^+$ (Calcd. 405.2036 for $C_{24}H_{30}O_4Na$).

Ferusingensine N (8): white amorphous powder; $[\alpha]_D^{20}$ +10.0 (*c* 0.40, MeOH); the ^1H and ^{13}C NMR ($CDCl_3$) data are detailed in Tables 2 and 3; the HR-ESI-MS at *m/z* 819.4074 $[2M+Na]^+$ (Calcd. 819.4077 for $C_{48}H_{60}O_{10}Na$).

Ferusingensine O (9): white amorphous powder; $[\alpha]_D^{20}$ −4.0 (*c* 0.65, MeOH); the ^1H and ^{13}C NMR ($CDCl_3$) data are provided in Tables 2 and 3; the HR-ESI-MS at *m/z* 399.2175 $[M+H]^+$ (Calcd. 399.2166 for $C_{24}H_{31}O_5$).

Cell culture

BV-2 microglial cells were cultured in DMEM supplemented with 10% fetal bovine serum (FBS), 2 mmol·L^{-1} glutamine, 100 U·mL^{-1} penicillin, and 100 μg·mL^{-1} streptomycin. The cells were maintained at 37 °C in a humidified atmosphere with 5% CO_2. Experiments were conducted using cells in the logarithmic phase of growth.

Measurement of cell viability

Cell viability was assessed using the MTT assay. BV-2 microglial cells were seeded into 96-well microtiter plates and treated with the test compounds for 24 h. Following the treatment, 0.25 mg·mL^{-1} MTT solution was added to each well, and the plates were incubated for an additional 4 h at 37 °C. After incubation, the supernatant was removed, and the formazan crystals formed by viable cells were dissolved in dimethyl sulfoxide (DMSO). The absorbance was measured at 490 nm using a plate reader (Bio-Tek, Winooski, VT, USA) [10].

Nitrite assay

Nitrite levels in the cell culture supernatants were determined using the Griess reagent method, as described by Li *et al*. [10]. BV-2 cells were seeded into 96-well microtiter plates and treated with compounds **1**–**9** and minocycline in the presence of lipopolysaccharide (LPS, 100 ng·mL^{-1}) for 24 h. After treatment, 50 μL of the culture supernatant was mixed with 50 μL of Griess reagent at room temperature. The absorbance was measured at 540 nm to quantify nitrite concentration.

Conclusion

SCs have been predominantly isolated from several taxonomically related plants of the *Ferula* genus and are fascinating candidates due to their wide range of anti-neuroinflammatory activities. This study employed a structure-guided separation approach to accurately isolate target SCs from the resin of the endangered plant *F. sinkiangensis*. Among the isolated compounds, Compounds **2**, **3**, and **6** demonstrated significant inhibition of NO production in LPS-stimulated BV2 microglial cells.

Supporting Information

The Supporting Information, including "S-Extraction and Isolation", 1D and 2D NMR, HR-ESI-MS, UV and IR spectra of compounds **1**−**9**, can be requested by sending E-mails to the corresponding authors.

References

[1] Guo TT, Zhou YP, Dang W, *et al*. "Preexistence" and "present life" of traditional Chinese medicine Ferulae Resina [J]. *Chin Tradit Herb Drugs*, 2021, **52**(17): 5401-5413.

[2] Julie C, Alice G, Catherine H, *et al*. Molecular and cellular neuroinflammatory statusof mouse brain after systemic lipopolysaccharide challenge: importance of CCR_2/CCL_2 signaling [J]. *J Neuroinflammation*, 2014, **11**: 132.

[3] Cheng XB, Zhao CL, Jin ZW, *et al*. Natural products: potential therapeutic agents for atherosclerosis [J]. *Chin J Nat Med*, 2022, **20**(11): 830-845.

[4] Li N, Guo TT, Zhou D. *Bioactive Sesquiterpene Coumarins From Plants. Studies in Natural Products Chemistry* [M]. Elsevier, 2018, **51**: 251-282.

[5] Zhang W, Mi Y, Jiao K, *et al*. Kellerin alleviates cognitive impairment in mice after ischemic stroke by multiple mechanisms [J]. *Phytother Res*, 2020, **34**(9): 2258-2274.

[6] Zhou J, Liu FJ, Li XX, *et al*. A strategy for rapid discovery of traceable chemical markers in herbal products using MZmine 2 data processing toolbox: a case of Jing Liqueur [J]. *Chin Herb Med*, 2021, **13**(3): 430-438.

[7] Tosun F, Beutler JA, Ransom TT, *et al*. Anatolicin, a highly potent and selective cytotoxic sesquiterpene coumarin from the root extract of *Heptaptera anatolica* [J]. *Molecules*, 2019, **24**(6): 1153-1161.

[8] Wang J, Huo X, Wang H, *et al*. Undescribed sesquiterpene coumarins from the aerial parts of *Ferula sinkiangensis* and their anti-inflammatory activities in lipopolysaccharide-stimulated RAW 264.7 macrophages [J]. *Phytochemistry*, 2023, **210**: 113664.

[9] Guo TT, Zhou D, Yang Y, *et al*. Bioactive sesquiterpene coumarins from the resin of *Ferula sinkiangensis* targeted on overactivation of microglia [J]. *Bioorg Chem*, 2020, **104**: 104338.

[10] Li J, Li N, Li X, *et al*. Characteristic alpha-acid derivatives from *Humulus lupulus* with antineuroinflammatory activities [J]. *J Nat Prod*, 2017, **80**(12): 3081-3092.

Cite this article as: DANG Wen, GUO Tingting, ZHOU Di, *et al*. Structure-guided isolation of anti-neuroinflammatory sesquiterpene coumarins from *Ferula sinkiangensis* [J]. *Chin J Nat Med*, 2024, **22**(7): 643-653.